volume of depolarization solution [10 mM Hepes (pH 7.4), 170 mM KCl, 1.3 mM $MgCl_2$, and 0.9 mM $CaCl_2$]. Control cultures were either untreated or treated with vehicle (water or dimethyl sulfoxide) or 0.41 volume of NaCl solution [10 mM Hepes (pH 7.4), 170 mM NaCl, 1.3 mM $MgCl_2$, and 0.9 mM $CaCl_2$]. To prevent excitotoxic cell death, sodium kynurenate (1 mM) and $MgCl_2$ (11.3 mM) (final concentrations) were added to the medium 10 minutes after stimulation. Total RNA was collected 50 minutes after stimulation and analyzed by Northern blot analysis.

9. H. Bading and M. E. Greenberg, unpublished observation.
10. P. I. Hanson and H. Schulman, *Annu. Rev. Biochem.* **61**, 559 (1992).
11. M. Sheng, M. A. Thompson, M. E. Greenberg, *Science* **252**, 1427 (1991); P. K. Dash, K. A. Karl, M. A. Colicos, R. Prywes, E. R. Kandel, *Proc. Natl. Acad. Sci. U.S.A.* **88**, 5061 (1991).
12. K. A. Ocorr and H. Schulman, *Neuron* **6**, 907 (1991); S. S. Molloy and M. B. Kennedy, *Proc. Natl. Acad. Sci. U.S.A.* **88**, 4756 (1991).
13. M. MacNicol, A. B. Jefferson, H. Schulman, *J. Biol. Chem.* **265**, 18055 (1990).
14. Labeling medium consisted of a mixture of buffered salt-glucose-glycine (SGG) solution [10 mM Hepes (pH 7.4), 114 mM NaCl, 26.1 mM $NaHCO_3$, 5.3 mM KCl, 1 mM $MgCl_2$, 2 mM $CaCl_2$, 30 mM glucose, 1 mM glycine, 0.5 mM sodium pyruvate, and 0.001 percent phenol red] and phosphate-free Eagle's minimum essential medium (MEM) (99:1 vol:vol), supplemented with insulin (7.5 μg/ml), transferrin (7.5 μg/ml), sodium selenite (7.5 ng/ml), penicillin G (50 U/ml), and streptomycin sulfate (50 μg/ml). Neurons were washed once in labeling medium and incubated in the same medium for 20 to 30 minutes at 37°C in an atmosphere of 7.5 percent CO_2 and 92.5 percent air. Subsequently, [^{32}P]orthophosphate (0.3 to 0.5 mCi/ml) was added to the medium. After 3 hours, the neurons were stimulated for 2 minutes with glutamate (10 μM) or 0.41 volume of KCl depolarization solution [10 mM Hepes (pH 7.4), 170 mM KCl, 1 mM $MgCl_2$, and 2 mM $CaCl_2$]. Cell lysis and immunoprecipitation with a mixture of two monoclonal antibodies to the α and β subunits of CaM kinase were done as described (*13*).
15. S. G. Miller and M. B. Kennedy, *Cell* **44**, 861 (1986); F. S. Gorelick, J. K. T. Wang, Y. Lai, A. C. Nairn, P. Greengard, *J. Biol. Chem.* **263**, 17209 (1988); P. I. Hanson *et al.*, *Neuron* **3**, 59 (1989).
16. H. Bading, D. D. Ginty, M. E. Greenberg, unpublished observation.
17. H. Van Belle, *Cell Calcium* **2**, 483 (1981).
18. H. Tokumitsu *et al.*, *J. Biol. Chem.* **265**, 4315 (1990).
19. Calmidazolium (5 μM) inhibited the increase in CaM kinase activity in response to KCl and glutamate by 41 ± 5 and 58 ± 14 percent, respectively (means ± SEM, $n = 3$); KN-62 (5 μM) inhibited the increase in CaM kinase activity in response to KCl and glutamate by 76 ± 11 and 67 ± 16 percent, respectively (means ± SEM, $n = 3$).
20. D. A. Greenberg, C. L. Carpenter, R. O. Messing, *Brain Res.* **404**, 401 (1987); P. A. Doroshenko, P. G. Kostyuk, E. A. Luk'yanetz, *Neuroscience* **27**, 1073 (1988); G. Li, H. Hidaka, C. B. Wollheim, *Mol. Pharmacol.* **42**, 489 (1992).
21. Transfection medium consisted of a mixture of SGG solution (*14*) and MEM (9:1 vol:vol), supplemented as described (*14*). A total of 3 μg of DNA [2 μg human c-*fos* plasmid and 1 μg of α-globin plasmid (*22*)], diluted in 0.1 ml of 0.15 M NaCl, was mixed with 0.1 ml of 0.15 M NaCl containing 160 μM dioctadecylamidoglycylspermine [J. P. Loeffler *et al.*, *J. Neurochem.* **54**, 1812 (1990)]. After a 10- to 15-minutes incubation at room temperature, the solution was diluted with 1.8 ml of transfection medium and added to one 60-mm dish of hippocampal neurons (8 days after plating) from which the growth medium had been removed. The neurons were maintained for 3 hours at 37°C in an atmosphere of 5 percent CO_2 and 95 percent air. The medium was then replaced with 3 ml of fresh transfection medium containing CNQX (40 μM). Stimulation of the neurons, 40 to 48 hours after transfection, was as described (*8*), except that the KCl depolarization solution contained 1 mM $MgCl_2$ and 2 mM $CaCl_2$. Total RNA was analyzed in RNase protection assays (*22*).
22. M. Sheng, S. T. Dougan, G. McFadden, M. E. Greenberg, *Mol. Cell. Biol.* **8**, 2787 (1988); M. Sheng, G. McFadden, M. E. Greenberg, *Neuron* **4**, 571 (1990).
23. The relative increase (mean ± SEM) in the amount of mRNA transcribed from plasmid pF222 normalized to the expression of α globin was 1.19 ± 0.16 in the presence of glutamate and nifedipine ($n = 4$) and 4.6 ± 1.14 after KCl-induced depolarization ($n = 4$).
24. V. M. Rivera and M. E. Greenberg, *New Biol.* **2**, 751 (1990); R. Treismann, *Sem. Cancer Biol.* **1**, 47 (1990).
25. H. Bading and M. E. Greenberg, *Science* **253**, 912 (1991).
26. H. Gille, A. D. Sharrocks, P. E. Shaw, *Nature* **358**, 414 (1992); V. M. Rivera, R. P. Misra, R.-H. Chen, J. Blenis, M. E. Greenberg, unpublished observation.
27. D. D. Ginty *et al.*, *Science* **260**, 238 (1993).
28. L. A. Berkowitz, K. T. Riabowol, M. Z. Gilman, *Mol. Cell Biol.* **9**, 4272 (1989).
29. R. P. Misra, C. K. Miranti, V. M. Rivera, M. E. Greenberg, unpublished observation.
30. C. M. Ely *et al.*, *J. Cell Biol.* **110**, 731 (1990).
31. R. Yuste and L. C. Katz, *Neuron* **6**, 333 (1991); A. Frandsen and A. Schousboe, *J. Neurochem.* **56**, 1075 (1991); H. Bading, N. J. Sucher, M. E. Greenberg, unpublished observation.
32. We thank M. M. Segal for help in culturing hippocampal neurons, H. Schulman for CaM kinase antibodies, and J. P. Loeffler for advice on the transfection technique. Supported by the Deutsche Forschungsgemeinschaft (H.B.), by NIH NRSA2F32 NS 08764, and American Heart Association, Mass Affiliate, 13-466-912 (D.D.G.), by NIH grant NS28829 (M.E.G.), and (to M.E.G.) an American Cancer Society Faculty Research Award (FRA-379) and a Scholar's Award from the McKnight Endowment Fund for Neuroscience.

31 August 1992; accepted 24 February 1993

Chips off of Asteroid 4 Vesta: Evidence for the Parent Body of Basaltic Achondrite Meteorites

Richard P. Binzel and Shui Xu

For more than two decades, asteroid 4 Vesta has been debated as the source for the eucrite, diogenite, and howardite classes of basaltic achondrite meteorites. Its basaltic achondrite spectral properties are unlike those of other large main-belt asteroids. Telescopic measurements have revealed 20 small (diameters ≤10 kilometers) main-belt asteroids that have distinctive optical reflectance spectral features similar to those of Vesta and eucrite and diogenite meteorites. Twelve have orbits that are similar to Vesta's and were previously predicted to be dynamically associated with Vesta. Eight bridge the orbital space between Vesta and the 3:1 resonance, a proposed source region for meteorites. These asteroids are most probably multikilometer-sized fragments excavated from Vesta through one or more impacts. The sizes, ejection velocities of 500 meters per second, and proximity of these fragments to the 3:1 resonance establish Vesta as a dynamically viable source for eucrite, diogenite, and howardite meteorites.

About 6 percent of the meteorites falling to Earth have an igneous composition indicative of an origin in lava flows or basaltic intrusions on other planetary bodies. Although a few individual basaltic achondrite meteorites are now generally recognized to have been derived from the moon and Mars (*1*), there remains a debate over the parent body for most of these meteorites: the eucrites, diogenites, and howardites (*2*). Compositionally, the eucrites have the characteristics of basalt, the diogenites are plutonic, and the howardites are polymict breccias consisting of eucrite and diogenite fragments.

Asteroid 4 Vesta has been at the center of the debate over the parent body of the howardite-eucrite-diogenite (HED) meteorites. Vesta's optical spectrum, first measured by McCord *et al.* (*3*), contains a strong absorption band attributed to pyroxene centered near 9000 Å. On the basis of comparison with laboratory spectra of basaltic achondrites and Apollo 11 lunar samples, McCord *et al.* concluded that Vesta's surface is basaltic. Subsequent researchers (*4*) have interpreted that Vesta has a differentiated basaltic crust composed of a Mg-rich and Ca-poor pigeonite. Vesta's spectrum and apparent basaltic achondrite composition is unlike those of any other large main-belt asteroids, over 500 of which have been investigated (*5*). Drake (*6*) thus argued that Vesta must be the source for the basaltic achondrite meteorites. However, apparent dynamical difficulties in delivering fragments from Vesta to the Earth have

The authors are in the Department of Earth, Atmospheric, and Planetary Sciences, Massachusetts Institute of Technology, Cambridge, MA 02139.

precluded any general consensus toward this conclusion (*7*, *8*). Vesta is far from dynamically favored meteorite source regions, the 3:1 Jovian and the ν_6 secular resonances, where asteroid orbits can dynamically evolve into Earth-crossing trajectories (*8*, *9*). Obtaining meteorite samples from Vesta requires a seemingly implausible first step in which large (kilometer-sized) fragments must be ejected with sufficient velocities to reach a resonance (*10*).

In this article, we report observational and dynamical evidence that large (multikilometer) fragments have been ejected from Vesta with significant velocities. This observation implies that substantial meteoroid parent body samples from Vesta can reach the resonances.

Observations. We have used high quantum efficiency charge-coupled device (CCD) detectors to survey the spectroscopic properties of main-belt asteroids having apparent magnitudes as faint as $m_v = 18$ and estimated diameters smaller than 10 km. In particular, we obtained spectra of 15 of the ~30 asteroids that have been proposed to be linked to Vesta as a dynamical family (*11*, *12*) and more than 80 other small main-belt asteroids in the region nearby Vesta (Fig. 1 and Tables 1 and 2). All observations were obtained with the 2.4-m Hiltner telescope of the Michigan–Dartmouth–Massachusetts Institute of Technology (MDM) Observatory (*13*) and were reduced to normalized reflection spectra with standard procedures (*14*).

In all, 12 of the observed Vesta family members and 8 of the other small main-belt asteroids sampled displayed basaltic achondrite spectra, characterized most notably by a strong absorption band near 9000 Å (Fig. 2 and 3). Fourteen of these (Fig. 2) are similar to Vesta, showing the spectral characteristics of eucrite meteorites with absorption band centers near 9400 Å. The only significant differences they show from Vesta's spectrum are steeper slopes shortward of 7500 Å, possibly attributable to slight variations in iron content. Particle size effects either from solid rock surfaces or particulate surface material might also produce the observed differences in band depths and spectral slopes. Such slope variations are readily seen in the class of eucrite meteorites (*15*).

The remaining six asteroids (Fig. 3), however, show more extreme basaltic achondrite features: Their spectra peak more sharply at a shorter wavelength and show a much deeper and less broad 9000 Å absorption band that is centered at a shorter wavelength than for eucrites. These characteristics are suggestive of diogenite basaltic achondrite meteorites. A positive relation to diogenites, however, must await additional spectroscopic measurements between 1.0 to 1.5 μm. At these wavelengths, diogenites are distinguished from eucrites by their lack of a weak feldspar absorption band. Because these spectra (Fig. 3) are visibly distinguishable from Vesta's overall spectrum and fall far from Vesta when translated into principal component space (*16*), we propose that these

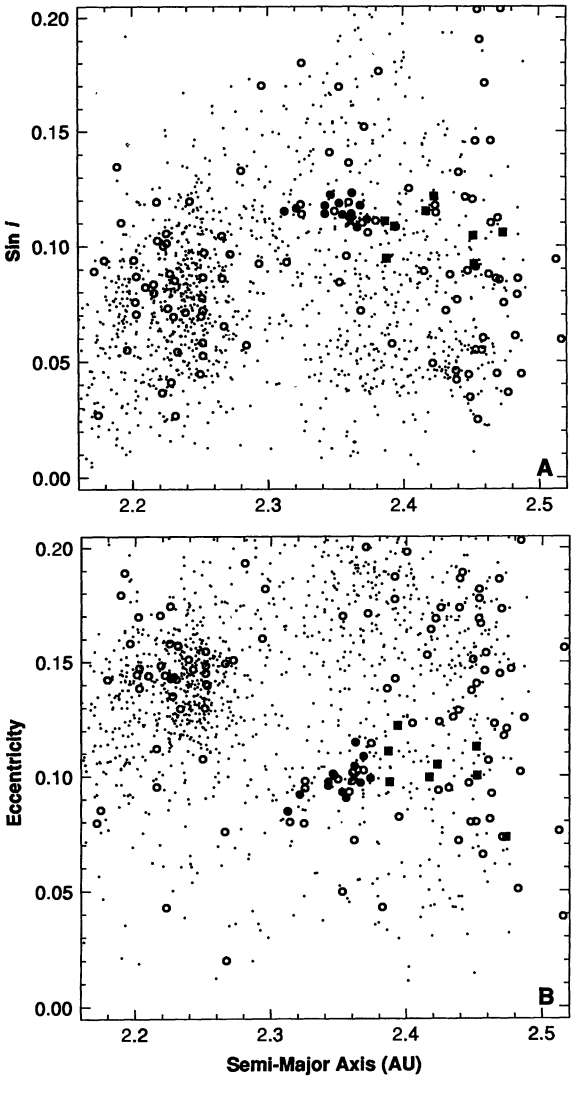

Fig. 1. Distribution of asteroids in proper orbital element space (*20*) in the inner main belt for (**A**) semimajor axis versus sin *i* (inclination) and (**B**) semimajor axis versus eccentricity. Vesta's position is denoted by an "X" (at 2.36 AU, sin *i* = 0.11, and eccentricity of 0.10). The symbol • indicates the positions for the 12 predicted Vesta family asteroids that we have observed to display basaltic achondrite spectra. Positions for asteroids that we have also observed, but which do not have spectral properties like basaltic achondrites are denoted by ○. Eight additional discovered basaltic achondrite asteroids, depicted by ■, bridge the region between Vesta and the 3:1 resonance Kirkwood gap (evidenced by the paucity of asteroids at 2.50 AU, right). These latter objects are found only within limited ranges of inclination and eccentricity that encompass Vesta.

Table 1. Summary of asteroid observations. The number of independent spectral image exposures, *N*, is given for each night.

Asteroid	Observation dates (UT)	*N*
4 Vesta	91/10/31	3
1273 Helma	93/01/21	2
1646 Rosseland	92/11/26	2
	92/11/27	2
1906 Naef	91/12/07	3
	91/12/08	4
	91/12/14	3
	91/12/15	6
1929 Kollaa	92/11/27	2
1933 Tinchen	92/09/06	2
	92/09/07	3
2011 Veteraniya	92/11/29	1
	92/11/30	1
	92/12/01	1
2024 McLaughlin	93/01/21	2
2113 Ehrdni	93/01/21	3
2442 Corbett	92/11/30	1
	92/12/01	1
2590 Mourao	92/11/26	3
3153 Lincoln	92/11/28	1
	92/12/01	1
3155 Lee	91/10/28	4
	91/10/29	3
3268 De Sanctis	92/03/11	2
3657 1978 ST6	92/09/06	2
	92/09/07	4
3869 Norton	92/03/11	2
	92/03/12	3
3944 Halliday	92/11/28	1
	92/11/29	2
	92/12/01	1
3968 Koptelov	92/09/06	3
4005 1972 TC2	91/12/07	2
	91/12/08	6
4038 Kristina	91/10/29	4
4147 Lennon	92/09/05	3
	92/09/06	3
4215 1987 VE1	93/01/21	2
4510 Shawna	93/01/21	1
4546 Franck	92/11/28	2

asteroids represent a new taxonomic class, which we denote by the letter J (mnemonic for the Johnstown diogenite meteorite).

Diogenites are plutonic rocks with coarse grain sizes formed, perhaps at substantial depths (*17*), during crystal accumulation in a subsurface magma chamber within a body having a eucritic surface. Large impacts could subsequently excavate diogenite samples. Gaffey (*18*) found at least one pyroxene-rich region on Vesta, which he interpreted as having a diogenite composition resulting from impact excavation.

Dynamics. Could large fragments, such as these basaltic achondrite asteroids, be excavated from Vesta? In our analysis we explicitly examined impacts as the likely excavation process.

For a fragment of mass m to escape a parent body's surface, its total kinetic energy E upon ejection must be greater than or equal to the potential energy needed to escape, E_{esc}. We denote $E_a = E_{esc} - E$ as the additional kinetic energy of the fragment beyond E_{esc}. Thus

$$\frac{1}{2} mv^2_{eject} = \frac{1}{2} mv^2_{esc} + \frac{1}{2} mv^2_a \quad (1)$$

where v_{eject} is the ejection velocity of the fragment, v_{esc} is the surface escape velocity for the parent body, and v_a is the scaler value for the additional velocity. For Vesta we assumed that the mean diameter is 520 km (*19*) and the mean density is 3.5 g cm^{-3}; for these values $v_{esc} = 365$ m s^{-1}. To compute the v_a that allows a fragment to achieve an independent heliocentric orbit, we first assume that the parent body has a circular orbit. The orbital velocity can be written as $v_{orb} = (GM/a)^{1/2}$, and for a small velocity change

$$\Delta v = -\frac{1}{2} (GM)^{1/2} a^{-3/2} \Delta a \quad (2)$$

where Δa is the change in semimajor axis a of the fragment's orbit with respect to the parent body and M is the solar mass. The planar tangential component of the fragment's additional velocity is given by $v_a = -\Delta v$, where for positive values of v_a (in the direction of the parent body's orbital velocity) the semimajor axis increases and v_{orb} decreases. The radial and out-of-plane components serve to change the fragment's orbital eccentricity (e) and inclination (i). For a parent body in an eccentric orbit, Δe and Δi for a fragment's orbit are highly sensitive to the position of the parent body at the time of ejection. Because Vesta has a modest orbital eccentricity (*20*), and because e and i are subject to secular perturbations, we cannot reliably use these orbital elements to compute specific values for v_a. Thus, $v_a = |\Delta v|$ represents our only reliable value for the magnitude of the additional velocity of any specific fragment. However it also represents a minimum for v_a, being based on only the planar tangential component. We choose to account for the existence of all three vector components by assuming that they are equal and obtain $v_a = 3^{1/2}|\Delta v|$ for the three-dimensional resultant, where ejection velocities based on this assumed isotropy should give a reliable average for a sample of fragments (Table 2). Individual ejection velocities for the isotropic and minimum velocity cases are thus estimated by:

$$v^2_{eject} = v^2_{esc} + \frac{3}{4} GMa^{-3} (\Delta a)^2$$

$$v^2_{min} = v^2_{esc} + \frac{1}{4} GMa^{-3} (\Delta a)^2 \quad (3)$$

The largest fragments excavated from a target body during an impact event are most likely spalls originating from the surface

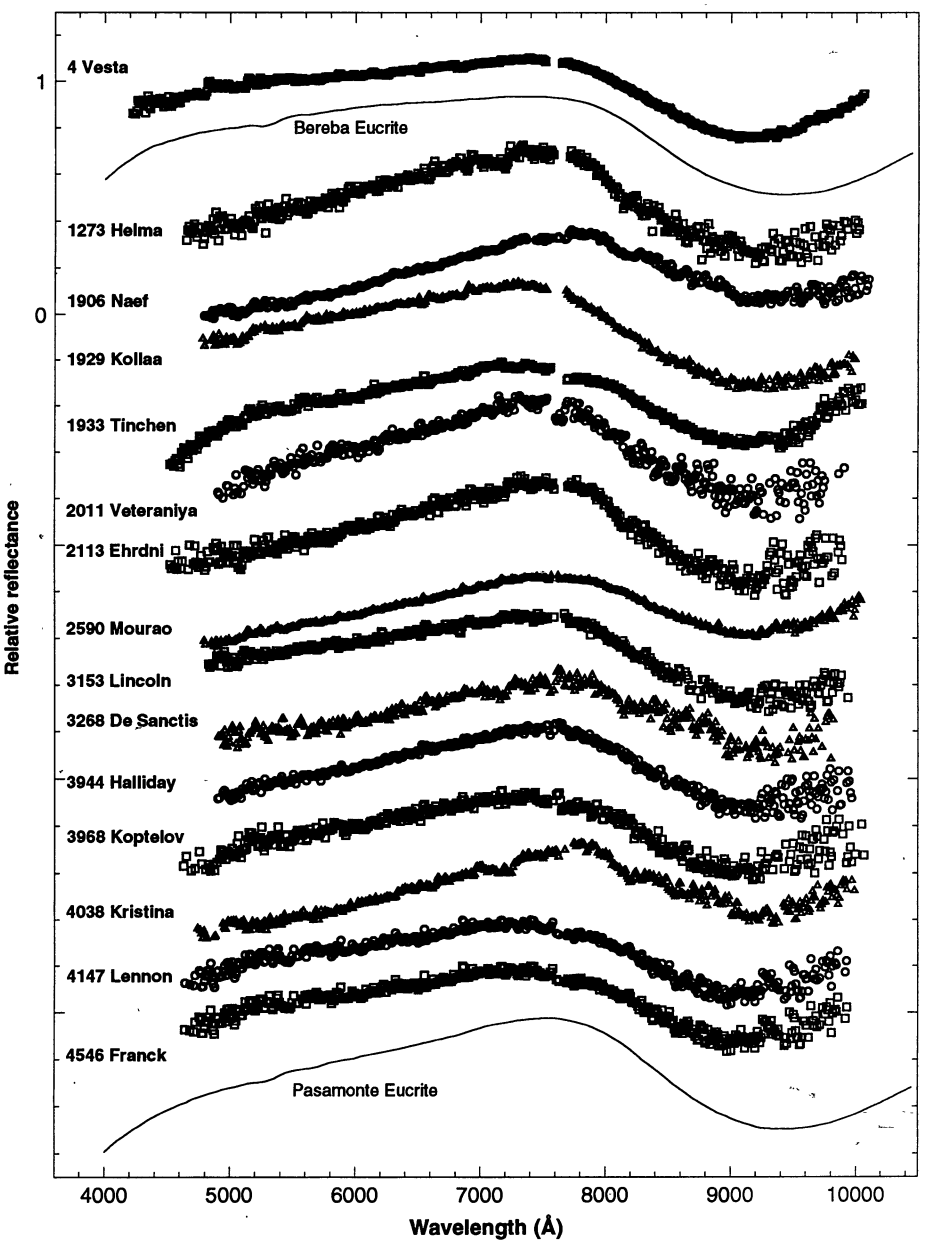

Fig. 2. Optical reflectance spectra for 14 asteroids (diameters 4 to 8 km) that display a deep absorption band near 9,000 Å, characteristic of basaltic achondrites. A spectrum of Vesta (diameter 520 km), obtained with the same instrumentation is included for comparison. Given that Vesta's spectrum is distinct among main-belt asteroids and the close dynamical relation of these small asteroids, they are almost certainly fragments excavated from Vesta's crust. Spectral characteristics for all of these asteroids fall within the range measured for eucrite meteorites, where measurements for Bereba and Pasamonte (solid lines) (*15*) are included for comparison. Asteroid 1929 Kollaa may contain some fraction of olivine, which could account for the onset of the absorption band shortward of 8,000 Å and the less steep upturn at 10,000 Å. All spectra have been normalized to unity at 5,500 Å and have been offset vertically for clarity.

near the impact point (*21*). We can relate the total volume of the spall fragments (V_{sp}) to the diameter of the impacting projectile (d) by:

$$\frac{V_{sp}}{d^3} = \frac{0.8\,\pi\,T}{\rho_T\,C_L\,v}\left[1 - \left(\frac{2\,v_{eject}}{v}\right)^{1/3}\right] \quad (4)$$

where T is the dynamic tensile strength of the target (taken to be 10^8 Pa), ρ_T is density of the target (assumed to be 3.5 g cm^{-3}), C_L is the wave propagation speed in the target (assumed to be 6 km s^{-1}), and v is the projectile impact velocity (*22*).

We estimated v following the methods described by Namiki and Binzel (*23*). From a bias-free set of 536 known asteroids larger than 30 km in diameter whose orbits currently cross that of Vesta, we determined the distribution of relative encounter velocities and collisional probabilities using the equations in (*24*). The mean encounter velocity was found to be 5.24 km s^{-1}, and the mean collisional probability was 5.90 × 10^{-18} km^{-2} yr^{-1} (Fig. 4).

We estimated V_{sp} from the basaltic achondrite asteroid diameters (Table 2); their total volume was equivalent to that of a sphere 8 km in radius. For their mean value, v_{eject} = 450 m s^{-1}, our solution of Eq. 4 implies that an impactor 130 km in diameter is required to produce this volume of spall fragments. If the remainder of the 30 or so predicted family members are also spall fragments from Vesta, then a 160-km impactor is required.

The sizes of the largest observed fragments and their ejection velocities can also be used as a constraint for impact dynamics models. For current models (*21*), the estimated maximum thickness of spall fragments (z_{sp}) is:

$$z_{sp} = \frac{T\,d}{\rho_T\,C_L\,v_{eject}} \quad (5)$$

We tested this relation using z_{sp} = 8 km as a boundary condition and 500 m s^{-1} as a representative ejection velocity based on the six largest fragments (Table 2). The result was that Eq. 5 unrealistically requires an impactor diameter larger than Vesta itself. If we allow that these Vesta fragments could be considerably elongated such that the spall thickness represents the smallest triaxial dimension (a speculation not based on light-curve information), a spall thickness of 2 to 3 km might be reasonable. For values of z_{sp} in this size range and an ejection velocity of 500 m s^{-1}, the required impactor diameter is 200 to 300 km.

How do these impactor sizes compare with the largest that Vesta can withstand? To investigate Vesta's survival, we used dimensionless pi-scaling (*25*). We followed the analysis in (*26*) to establish a disruption criterion that the excavated volume equals the total volume of the target. For this criterion, Vesta could survive the impact of a projectile 240 km across, and therefore likely survive the impact events suggested by spallation models.

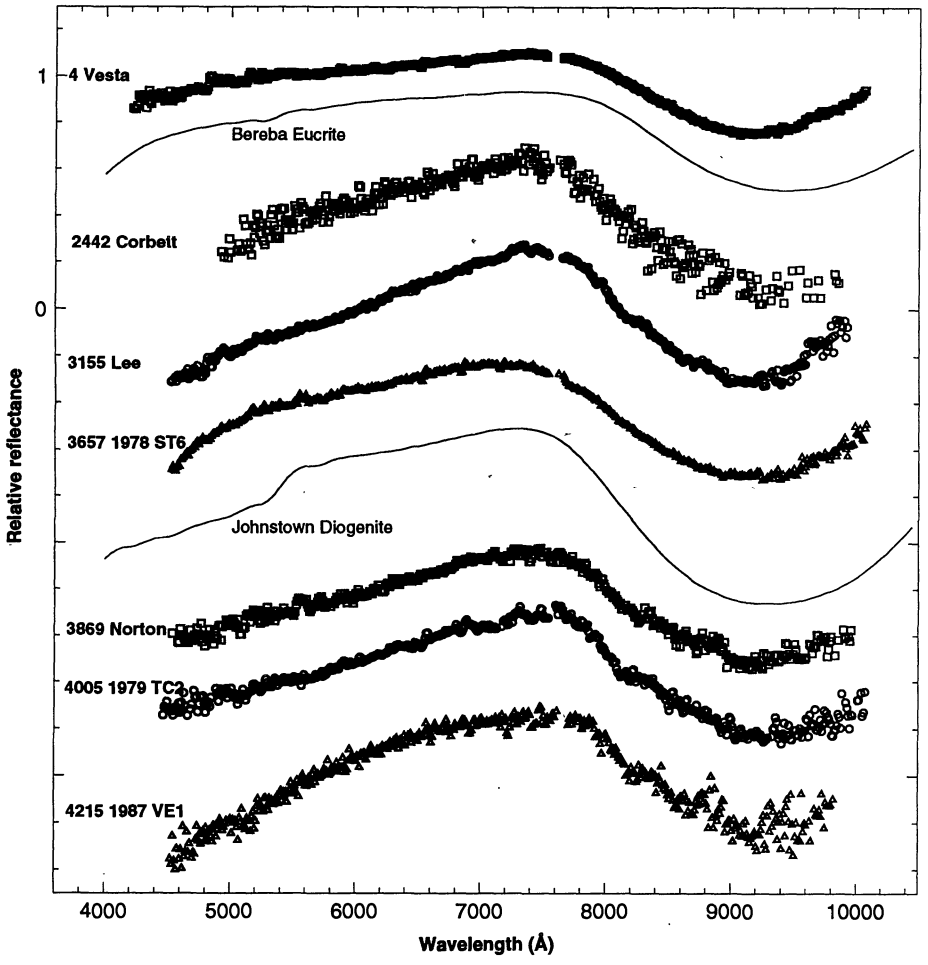

Fig. 3. Optical reflectance spectra for six additional basaltic achondrite main-belt asteroids (diameters 6 to 10 km). Vesta and the Bereba eucrite meteorite are included for comparison. Compared with eucrite spectra, these asteroids show steeper slopes below 7,500 Å, sharper peaks, and deeper 9,000 Å absorption bands centered at a shorter wavelength. Their spectral properties are more analogous to the diogenite class of basaltic achondrite meteorites. A spectrum of the Johnstown diogenite meteorite (*15*) is included for comparison. A new taxonomic class J is proposed for diogenite-analog asteroids. Asteroid 2442 Corbett may contain some fraction of olivine, which could account for the less steep upturn at 10,000 Å. All spectra have been normalized to unity at 5,500 Å and have been offset vertically for clarity.

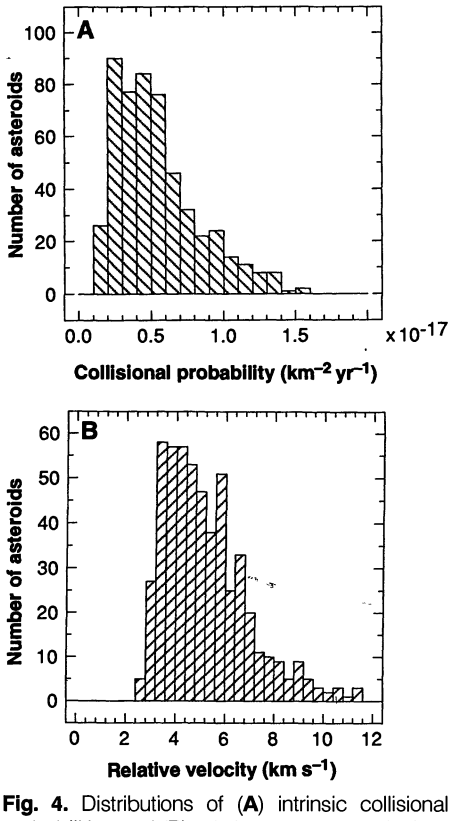

Fig. 4. Distributions of (**A**) intrinsic collisional probabilities and (**B**) relative encounter velocities for 536 numbered asteroids (diameters ≥30 km) whose orbits intersect Vesta's, computed using the methods of Namiki and Binzel (*23*). Their mean collisional probability is 5.90 × 10^{-18} km^{-2} yr^{-1} and mean relative velocity is 5.24 km s^{-1}.

Links to Vesta and implications. The circumstantial evidence linking the 12 Vesta family basaltic achondrite asteroids to Vesta appears to be overwhelming. Their mean orbital velocities are all within 200 m s^{-1} of Vesta and their spectral properties are distinctive and match those of Vesta (*18*). These observations thus establish confirmed members of the previously proposed Vesta family (*11, 12*).

Are the eight other basaltic achondrite asteroids that bridge the region between Vesta and the 3:1 resonance (Fig. 1 and Table 2) also genetically related to Vesta? The observations lead us to argue in favor of such a link for three reasons. First, they are spectrally indistinguishable from the confirmed Vesta family members and Vesta itself. Second, all of their orbits cross that of Vesta. Third, these additional basaltic achondrite fragments are found to have nearly equal orbital inclinations with Vesta and also have similar orbital eccentricities (Fig. 1). This last argument establishes a strong dynamical constraint in that for an object launched from a parent body with a velocity v_{eject}, the changes in eccentricity and inclination scale proportional to v_{eject}/v_{orb} and $\tan^{-1}(v_{eject}/v_{orb})$, respectively. For Vesta's heliocentric orbital velocity of 19.4 km s^{-1}, the maximum inferred ejection velocity of 0.88 km s^{-1} (if optimally directed) would change e or sin i values by about 0.05 from those of Vesta itself. For all eight asteroids, these elements are within 0.03 of Vesta's values.

How likely is it that the orbital element similarities between Vesta and the near-resonance basaltic achondrites are due to random chance? Over the semimajor axis range of 2.38 to 2.50 AU, we have sampled 50 asteroids. For the case of sin i, 22 are within ±0.03 AU of Vesta; thereby, the probability is 44 percent (22/50) that any one basaltic achondrite would fall in this range. The probability that all eight discovered basaltic achondrites would fall within this range of Vesta is therefore 0.44^8, or 0.2 percent. For the case of eccentricity, the analogous individual and group probabilities are 48 percent and 0.3 percent. The combined random probability for the observed coincidence in both orbital elements is thus only 0.06 percent.

The conclusions that the family and near-resonance basaltic achondrite asteroids are derived from Vesta pose a challenge for impact mechanics models to demonstrate that fragments 4 to 10 km across can be produced with ejection velocities of at least 500 m s^{-1}. Current spallation models seem to require nearly catastrophic impacts into Vesta to generate such fragment sizes and velocities. Such impacts are unlikely to have occurred if Vesta's observed eucritic crust is relatively thin, as the spectral signature of this crust could not have been retained in the face of a consequent disorganized reaccumulation (*27*). If Vesta's eucritic crust has substantial thickness (*17*), the constraint against it having experienced a nearly catastrophic impact is less severe. The largest observed eucritic fragment (10 km) sets a lower limit on the crustal thickness. Possible resolution to this problem may come from spallation models that allow for a target to be previously fractured or to be inhomogeneous with a lower density crust overlaying a higher density mantle. Such a model may allow thicker spall fragments to be produced from modest impacts.

Crater studies of the moon and terrestrial planets also suggest evidence for the ability of impacts to produce large ejecta units with high velocities. For the 93-km lunar crater Copernicus, several large secondary craters are inferred to have been formed from impact of 1- to 2-km fragments ejected at 500 m s^{-1}

Table 2. Summary of dynamical and physical properties for observed Vesta family members and near-resonance asteroids. Basaltic achondrite asteroids are classified as V or J (new class proposed here) on the basis of their eucrite-like or diogenite-like spectra. Their diameters are based on absolute magnitudes (H) and an assumed albedo of 0.38, the IRAS measured value for Vesta. Vesta's diameter is based on occultation results (*19*). Proper elements are from (*20*). Separate columns list the predicted family identifications (*11, 12*). Z31 and W169 denote the Vesta family. Z35 and W196 denote the Tinchen family, predicted to be related to Vesta. W165 refers to the Ausonia family (*12*). Three predicted Vesta-related asteroids, 1646, 2024, and 4510, have compositional classes unlike Vesta and are likely interlopers (*31*). Velocity estimates (derived in the text) are given for probable Vesta fragments. The last entries give velocities necessary for fragments from Vesta to reach the 3:1 and ν_6 resonances.

Asteroid	Diameter (km)	Proper elements			Families	Class	v_a (m s^{-1})	v_{eject} (m s^{-1})	v_{min} (m s^{-1})
		a	e	sin i					
Observed Vesta family members									
4 Vesta	520	2.36154	0.0994	0.1106	Z31 W169	V			
1646 Rosseland	26	2.36030	0.1015	0.1363	W169	C			
1906 Naef	6	2.37362	0.0990	0.1116	Z31 W169	V	86	375	368
1929 Kollaa	8	2.36260	0.1147	0.1230	W165	V	8	365	365
1933 Tinchen	6	2.35296	0.0933	0.1169	Z35 W196	V	61	370	367
2024 McLaughlin	10	2.32540	0.0945	0.1139	Z35 W196	A			
2590 Mourao	6	2.34250	0.0958	0.1174	Z35 W196	V	135	389	373
3155 Lee	7	2.34263	0.0974	0.1165	Z35 W196	J	134	389	373
3268 De Sanctis	5	2.34680	0.1002	0.1223	Z35 W169	V	105	380	370
3657 1978 ST6	7	2.31262	0.0882	0.1146	W196	J	348	504	417
3944 Halliday	5	2.36840	0.1085	0.1177	W165	V	49	368	366
3968 Koptelov	7	2.32151	0.0928	0.1180	Z35 W196	V	284	463	400
4038 Kristina	4	2.36618	0.0987	0.1102	Z31 W169	V	33	366	365
4147 Lennon	6	2.36197	0.1027	0.1141	Z31 W169	V	3	365	365
4510 Shawna	7	2.36000	0.0977	0.1189	Z31 W169	S			
4546 Franck	4	2.35560	0.0905	0.1136	Z31 W196	V	42	367	366
Basaltic achondrites discovered between Vesta and the 3:1 resonance									
1273 Helma	6	2.39370	0.1222	0.1085		V	229	431	388
2011 Veteraniya	6	2.38695	0.1108	0.1109		V	181	407	380
2113 Ehrdni	5	2.47380	0.0731	0.1057		V	798	877	588
2442 Corbett	6	2.38767	0.0974	0.0945		J	186	410	380
3153 Lincoln	5	2.42290	0.1049	0.1216		V	436	569	443
3869 Norton	6	2.45247	0.1002	0.0921		J	646	742	522
4005 1979 TC2	7	2.45195	0.1128	0.1045		J	642	739	520
4215 1987 VE1	10	2.41710	0.0993	0.1151		J	395	538	430
3:1 Resonance		2.50					984	1049	675
ν_6 Resonance		2.18					1290	1341	829

(*28*). Secondary craters related to the 225-km crater Mozart on Mercury were likely formed from fragments 2 to 4 km across ejected at similar velocities (*29*). For these secondary crater progenitors, it remains an open question whether they were coherent intact fragments or clumps of ejecta. Analogously for the discovered basaltic achondrite asteroids, it is uncertain whether they are intact fragments or rubble pile accumulations. The latter could form from proximate material having nearly identical ejection velocities that is able to re-accrete through self-gravity into bodies whose ultimate sizes are substantially greater than that of the largest intact fragment.

Finally, the discovery of basaltic achondrite asteroids spanning the region between Vesta and the 3:1 resonance provides a trail of evidence for a dynamical link between Vesta and basaltic achondrite meteorites. Equation 5 suggests that the sizes of spalled fragments are inversely proportional to their ejection velocities. Based on the mean ejection velocity of 590 m s^{-1} for the eight near-resonance fragments with diameters of 5 to 10 km, many more numerous meteoroid parent body fragments (0.1 to >1 km) could be ejected from Vesta with velocities exceeding the 700 to 1000 m s^{-1} necessary to fall within the 3:1 resonance. Velocities 200 to 300 m s^{-1} higher could allow Vesta fragments to reach the ν_6 resonance. These scaling arguments make it plausible that the three known V-type near-Earth asteroids with diameters of 1 to 4 km (*30*) are derived from Vesta. Injection of such large fragments to the resonances for subsequent delivery to the inner solar system is a critical step toward yielding a measurable sample of meteorites (*10*).

REFERENCES AND NOTES

1. U. B. Marvin, *Smithson. Contrib. Earth Sci.* **26**, 95 (1984); H. Y. McSween, *Rev. Geophys.* **23**, 391 (1985).
2. H. Y. McSween and E. Stolper, *Sci. Am.* **242**, 54 (June 1980).
3. T. B. McCord, J. B. Adams, T. V. Johnson, *Science* **168**, 1445 (1970).
4. H. P. Larson and U. Fink, *Icarus* **26**, 420 (1975).
5. For example, B. Zellner, D. J. Tholen, E. F. Tedesco, *ibid.* **61**, 355 (1985).
6. M. J. Drake, in *Asteroids*, T. Gehrels, Ed. (Univ. of Arizona Press, Tucson, 1979), pp. 765–782.
7. G. W. Wetherill, in "Asteroids: An Exploration Assessment" (*NASA Conf. Publ. 2053*, NASA, Houston, TX, 1978), pp. 17–35.
8. G. W. Wetherill, *Philos. Trans. R. Soc. London Ser. A* **323**, 323 (1987).
9. J. Wisdom, *Nature* **315**, 731 (1985).
10. R. Greenberg and C. R. Chapman, *Icarus* **55**, 455 (1983); G. W. Wetherill, *Meteoritics* **20**, 1 (1985); R. Greenberg and M. C. Nolan, in *Asteroids II*, R. P. Binzel, T. Gehrels, M. S. Matthews, Eds. (Univ. of Arizona Press, Tucson, 1989), pp. 778–804.
11. V. Zappalà, A. Cellino, P. Farinella, Z. Knezevic, *Astron. J.* **100**, 2030 (1990). Also V. Zappalà and A. Cellino, personal communication.
12. J. G. Williams, in *Asteroids*, T. Gehrels, Ed. (Univ. of Arizona Press, Tucson, 1979), pp. 1040–1063; in *Asteroids II*, R. P. Binzel, T. Gehrels, M. S. Matthews, Eds. (Univ. of Arizona Press, Tucson, 1989), pp. 1034–1072; *Icarus* **96**, 251 (1992); personal communication.
13. The MDM Observatory is located at Kitt Peak, Arizona. For our observations we used the MDM MKIII spectrograph. The combination of a 150-line-per-millimeter grism (blazed at 7300 Å) and a TI-4849 CCD detector (398 by 598 pixels, dispersion along the long axis) allowed first-order spectral coverage to be obtained over the interval of 4000 to 10000 Å with a dispersion of 10 Å per pixel. Order overlap was eliminated by placing a piece of Wratten 22 filter (cutting off wavelengths <5500 Å) over the red dispersion half of the CCD.
14. The measured asteroids were selected from those that were available for observation at the time of our telescope allocations. Our observing procedures were as follows. For faint program objects our standard exposure time was 900 s, where this value was chosen to limit the collection of cosmic rays in any individual image. Multiple exposures were obtained, reduced independently, and combined to achieve the final spectrum. Typically, the response of the CCD and the transmission of the telescope provided a signal-to-noise ratio of >20 for individual pixels in the final spectrum over the range of 4800 to 10,000 Å. Before and after each observation, we also observed a spectral standard star and often a bright asteroid having a known compositional type. These objects were reduced simultaneously with the program objects and then compared with published spectrophotometry (*5*) to assess the presence of systematic errors. We achieved solar analog calibration by observing either of the stars Hyades 64 or 16 Cyg B. Calibrating bias frames, flat-field images, and lamp spectra were all obtained using the identical instrument configuration. Under typical seeing conditions of 1 to 2 arc sec, a slit size of 5 arc sec (oriented north-south) was used. With rare exceptions, all observations were performed within 2 hours of the meridian and at air masses <1.3. Differential dispersion for the wavelength range covered was less than 1 arc sec, substantially smaller than the size of the slit. We reduced each spectral exposure using utilities in the Image Reduction and Analysis Facility (IRAF) software package developed by the National Optical Astronomy Observatories (NOAO). These procedures include the elimination of cosmic rays, bias subtraction, flat fielding, spectral extraction, sky subtraction, wavelength calibration, extinction correction, and flux calibration. The calibrated asteroid spectra were divided by the spectrum of the solar analog star and normalized to unity at 5500 Å.
15. M. J. Gaffey, *J. Geophys. Res.* **81**, 905 (1976).
16. D. J. Tholen, personal communication; ——— and M. A. Barucci, in *Asteroids II*, R. P. Binzel, T. Gehrels, M. S. Matthews, Eds. (Univ. of Arizona Press, Tucson, 1989), pp. 298–315.
17. T. L. Grove and K. S. Bartels, *Proc. Lunar Planet. Sci.* **22**, 437 (1992).
18. M. J. Gaffey, *Lunar Planet. Sci. Conf.* **XIV**, 231 (1983).
19. D. W. Dunham, *Occultation Newsl.* **V**, 93 (1991).
20. A. Milani and Z. Knezevic, *Icarus* **98**, 211 (1992).
21. H. J. Melosh, *ibid.* **59**, 234 (1984).
22. ———, *Geology* **13**, 144 (1985).
23. N. Namiki and R. P. Binzel, *Geophys. Res. Lett.* **18**, 1155 (1991).
24. G. W. Wetherill, *J. Geophys. Res.* **72**, 2429 (1967).
25. H. J. Melosh, *Impact Cratering: A Geologic Process* (Oxford Univ. Press, New York, 1989).
26. W. B. Tonks and H. J. Melosh, *Icarus* **100**, 326 (1992).
27. D. R. Davis, D. R. Chapman, S. J. Weidenschilling, R. Greenberg, *ibid.* **62**, 30 (1985).
28. A. M. Vickery, *ibid.* **67**, 224 (1986).
29. A. M. Vickery, *Geophys. Res. Lett.* **14**, 726 (1987).
30. D. Cruikshank, D. J. Tholen, W. K. Hartmann, J. F. Bell, R. H. Brown, *Icarus* **89**, 1 (1991).
31. The A-type classification for asteroid 2024 McLaughlin may reflect an abundant olivine composition, as might be found in the mantle of Vesta.

32. Data reported in this paper were obtained at the Michigan–Dartmouth–Massachusetts Institute of Technology Observatory. We thank V. Zappalà, A. Cellino, and J. Williams for encouragement and recommending targets. We thank M. Gaffey for providing his meteorite spectra in digital form. S. J. Bus provided assistance with the 1993 observations. Supported by NASA grant NAGW1450, a Presidential Young Investigator Award (R.P.B.), and a 1991–1992 Fullam/Dudley award (R.P.B.).

4 November 1992; accepted 5 February 1993